Electronic Supplementary Information

Edge and bridge engineering mediated exciton dissociation and charge separation in carbon nitride for boosting photocatalytic H$_2$ evolution integrated with selective amines oxidation

Meiyang Song,[#,a] Xiaoxu Deng,[#,b] Gen Li,[a] Qiuchen Wang,[a] Haiyan Peng,[a] Peng Chen[*,a] and Shuang-Feng Yin[*,c]

[a] Provincial Guizhou Key Laboratory of Green Chemical and Clean Energy Technology, School of Chemistry and Chemical Engineering, Guizhou University, Guiyang 550025, Guizhou, China

[b] College of Big Data and Information Engineering, Guizhou University, Guiyang 550025, Guizhou, China

[c] State Key Laboratory of Chemo/Biosensing and Chemometrics, Provincial Hunan Key Laboratory for Cost-effective Utilization of Fossil Fuel Aimed at Reducing Carbon-dioxide Emissions, College of Chemistry and Chemical Engineering, Hunan University, Changsha 410082, Hunan, China

[#] These authors contribute equally to this work

Email: pchen3@gzu.edu.cn (P. Chen), sf_yin@hnu.edu.cn (S. F. Yin).

Table S1. Binding energy and area ratio of C 1s over as prepared samples

Samples	C-NH		C=C/C-C		N=C-N		C=O	
	BE eV	Area ratio %	BE eV	Area ratio %	BE eV	Area ratio %	BE eV	Area ratio %
C_3N_4	286.2	2.0	284.6	5.9	288.0	92.1		
EBCN-1	286.1	5.7	284.6	11.1	288.0	60.4	288.5	22.8
EBCN-2	286.8	5.7	284.6	7.4	288.0	72.5	288.4	14.4
EBCN-3	286.2	3.5	284.6	7.6	287.9	76.6	288.5	12.3
ECN	286.2	5.1	284.6	10.7	288.0	67.4	288.5	16.8
BCN	286.2	6.2	284.6	52.2	287.9	41.6		

Table S2. Binding energy and area ratio of N 1s over as prepared samples

Samples	C-N=C		N-$(C)_3$		N-H_X	
	BE eV	Area ratio	BE eV	Area ratio	BE eV	Area ratio
C_3N_4	398.5	74.7	399.9	17.0	401.1	8.3
EBCN-1	398.5	66.0	399.7	21.3	401.0	12.7
EBCN-2	398.6	72.9	399.9	19.3	401.1	7.8
EBCN-3	398.3	64.6	399.5	29.3	400.7	6.1
ECN	398.2	75.3	399.9	13.3	400.9	11.4
BCN	397.9	86.2	399.7	6.5	400.5	7.3

Table S3. Binding energy and area ratio of O 1s over as prepared samples

Samples	Adsorbed oxygen		C=O		Adsorbed H_2O	
	BE	Area	BE	Area	BE	Area
	eV	ratio	eV	ratio	eV	ratio
EBCN-1	530.7	25.3	531.6	35.2	532.7	39.5
EBCN-2	530.6	26.1	531.6	34.7	532.7	39.2
EBCN-3	530.9	26.4	531.7	24.4	532.5	49.2
ECN	530.7	36.8	531.7	41.3	532.7	21.9

Table S4. Zeta potentials of the as-prepared photocatalysts.

Test time	EBCN-1 (mV)	EBCN-2 (mV)	EBCN-3 (mV)	C_3N_4 (mV)	ECN (mV)	BCN (mV)
1	-49.1	-60.3	-52.9	-43.2	-44.9	-42.5
2	-48.5	-62.5	-55.4	-45.6	-45.4	-43.6
3	-49.8	-59.5	-51.8	-46.3	-49.5	-40.9
4	-48.2	-60.5	-53.8	-44.5	-46.2	-39.1
5	-47.9	-63.8	-53.4	-47.3	-44.3	-40.2
6	-50.6	-59.4	-53.1	-47.2	-44.7	-40.8
Average	-49.0	-61.0	-53.4	-45.7	-45.8	-41.2.

Table S5. Comparison of the EBCN-2 photocatalysts with the previously reported ones for hydrogen production coupled with selective oxidation of benzylamine.

Entry	Catalyst	Reaction Conditions	H_2 production ($\mu mol \cdot g^{-1} \cdot h^{-1}$)	Ref. No.
1	EBCN-2	20 mg catalyst 10 mL BA 50 mL H_2O 1 mL H_2PtCl_6 300 W Xe lamp	2296.3	This work
2	Pt/PCN-777	10 mg catalyst 50 μL BA 50 μL H_2O 5mL DMF 300 W Xe lamp	332	[S1]
3	Pt/MOF-808	10 mg catalyst 50 μL BA 50 μL H_2O 5mL DMF 200mg $AgNO_3$ 300 W Xe lamp	1.7	[S1]
4	PdS_{A+C}/TiO_2-V_o	10 mg catalyst 500 $\mu L H_2O$ 500 μL BA 50 mL DMF 300 W Xe lamp	585.4	[S2]
5	$CdS/Ti_3C_2T_x$	10 mg catalyst 2.5 mmol H_2O 0.5 mmol BA 5 mL DMF 300 W Xe lamp	219.7	[S3]
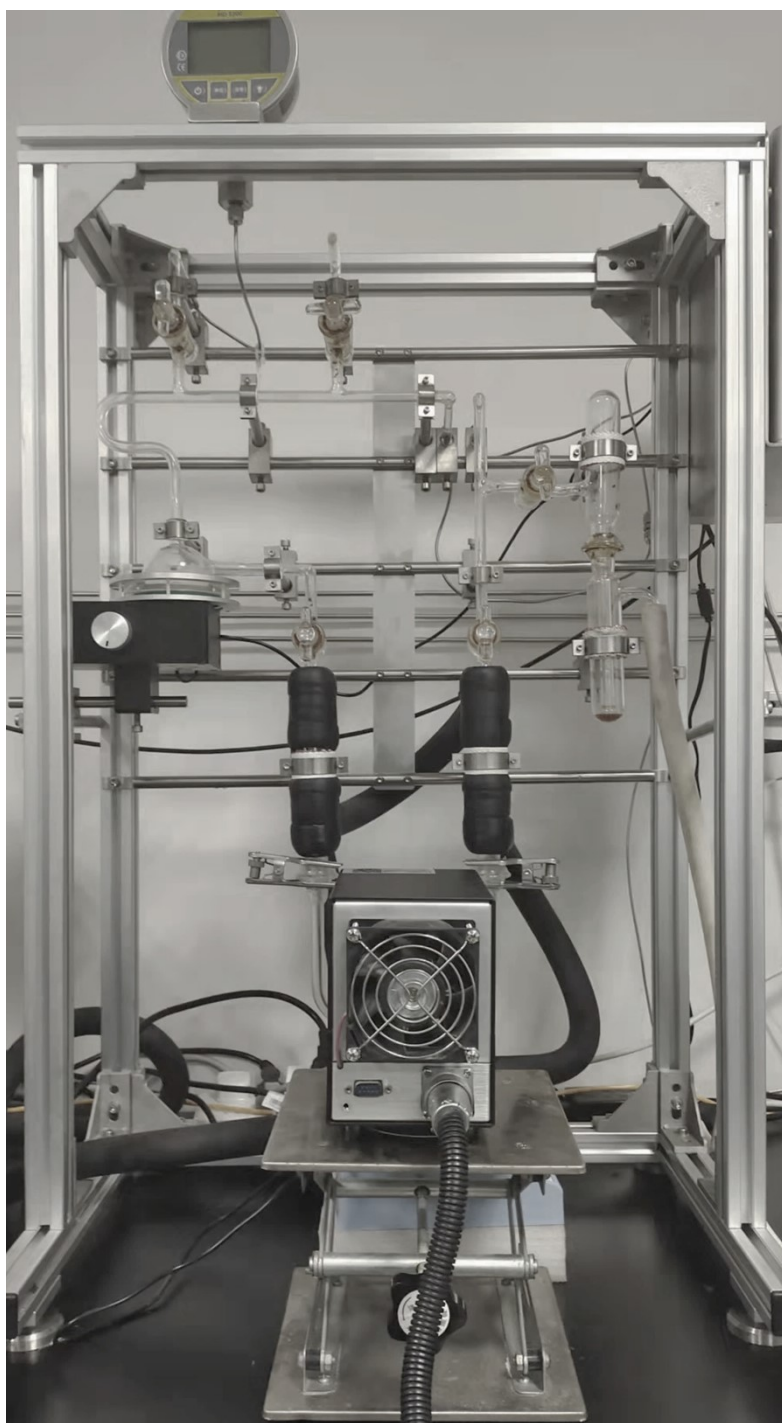
Fig. S1. Photograph of the multi-channel photocatalytic reaction system.
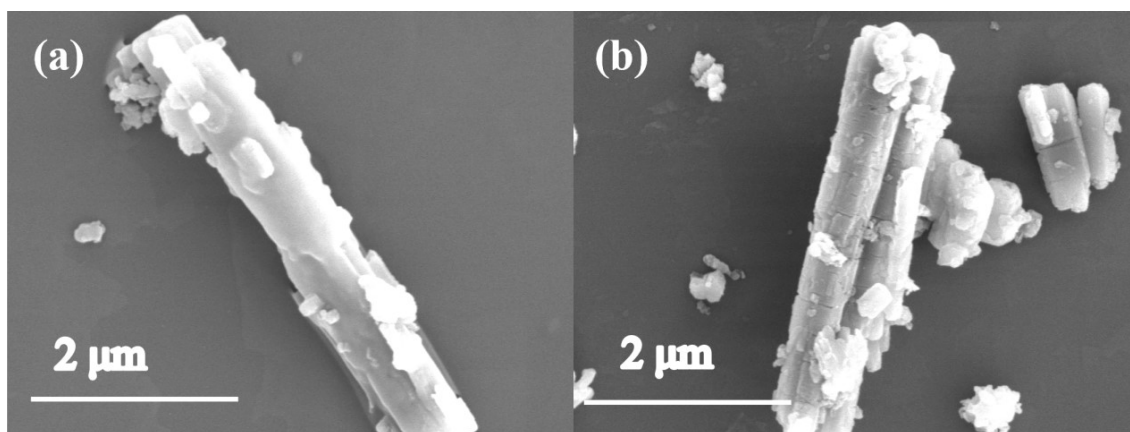
Fig. S2. SEM images of (a) melem and (b) precursor.
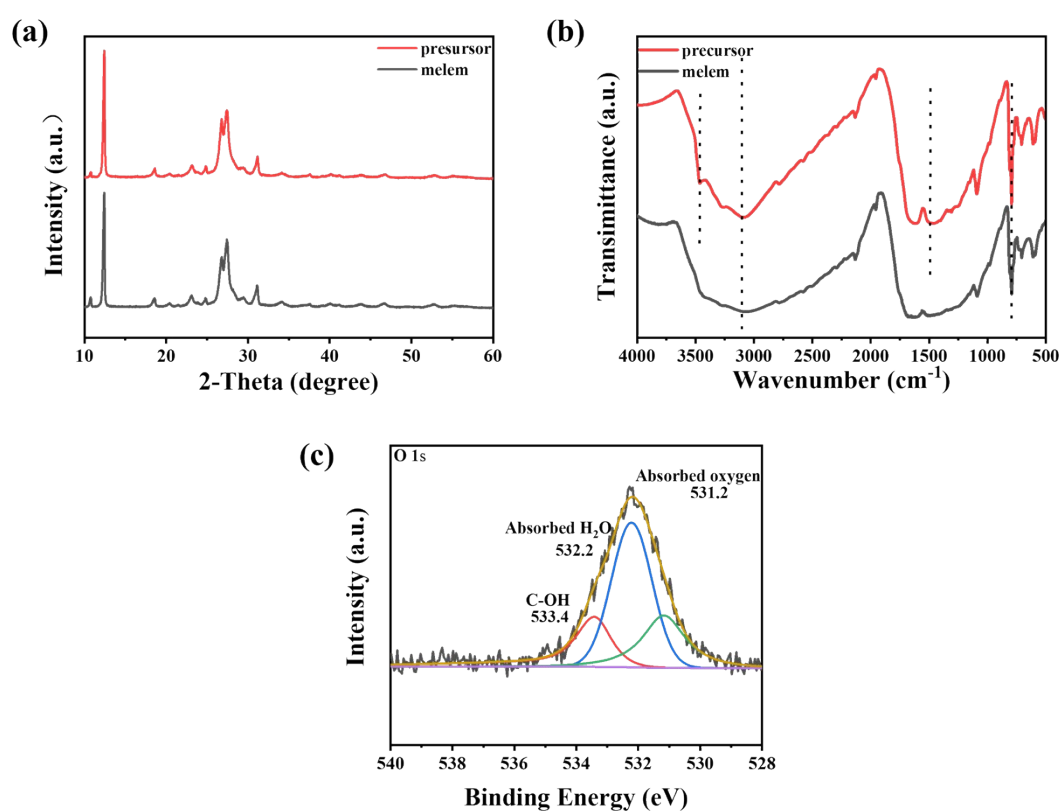
Fig. S3. (a) XRD patterns and (b) FTIR spectra of melem and precursor. (c) O 1s high-resolution spectra of precursor.

The XRD pattern of the as-synthesized precursor, depicted in **Fig. S3a**, is similar to the melem, which indicates that the formation of the precursor did not disrupt the structure of the melem.[S4] As shown in **Fig. S3b**, the peaks at 793.5 and 3103 cm^{-1}, corresponding to the vibration of triazine rings and the N-H group. Compared with the

result for melem, the FTIR spectrum of the precursor shows a new peak at 3465 cm^{-1} is the superposition absorption peak of a hydroxyl group, and the peak at 1495 cm^{-1} belongs to C-H$_2$, indicating that the N-H, C-H$_2$ and O-H groups exist in the precursor.[S5,6] **Fig. 3c** shows the O 1s spectra of the precursor at 531.2, 532.2 and 533.4 eV, which is related to the absorbed oxygen, absorbed H$_2$O and C-OH bonds, further confirmed that the structure of the precursor.[S7]
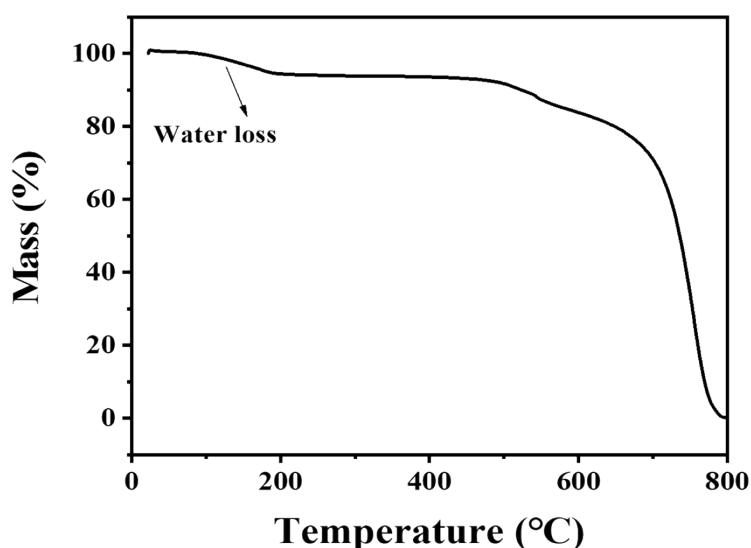
Fig. S4. TG spectrum of precursor.

The thermal behavior of the precursor was investigated using TGA technology, and the results are shown in **Fig. S4**. The TGA thermogram of the precursor shows two states of weightlessness in the range of 100-200°C and 450-740°C. The first small weight loss (~6%) in the range of 100-150°C was due to the loss of surface adsorbed water molecules. The second major weight loss started at 450°C, which is due to the gradual polymerization of the precursor.[S8]
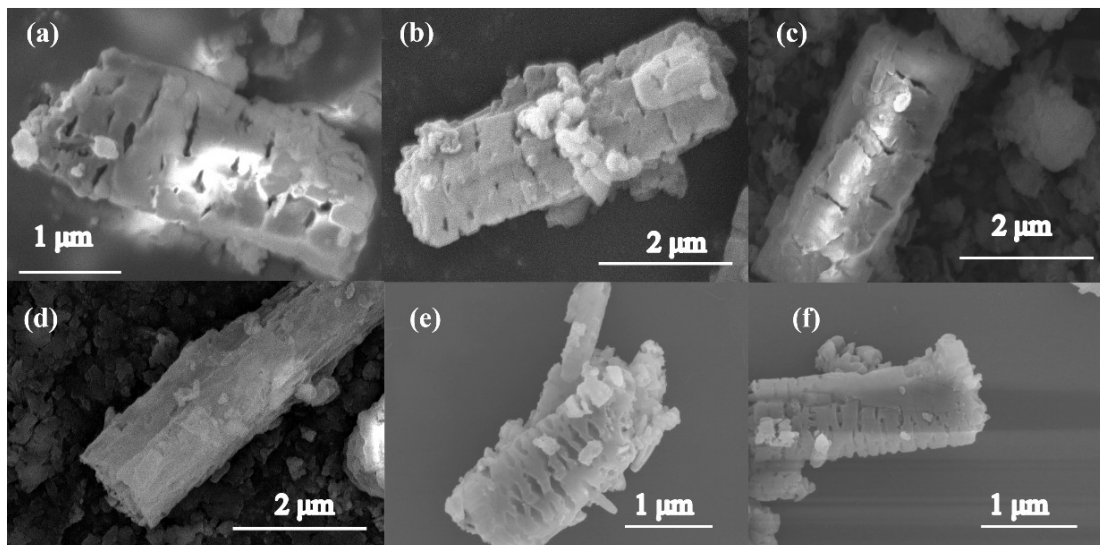
Fig. S5. SEM images of (a) EBCN-1, (b) EBCN-2, (c) EBCN-3, (d) C_3N_4, (e) ECN and

(f) BCN.
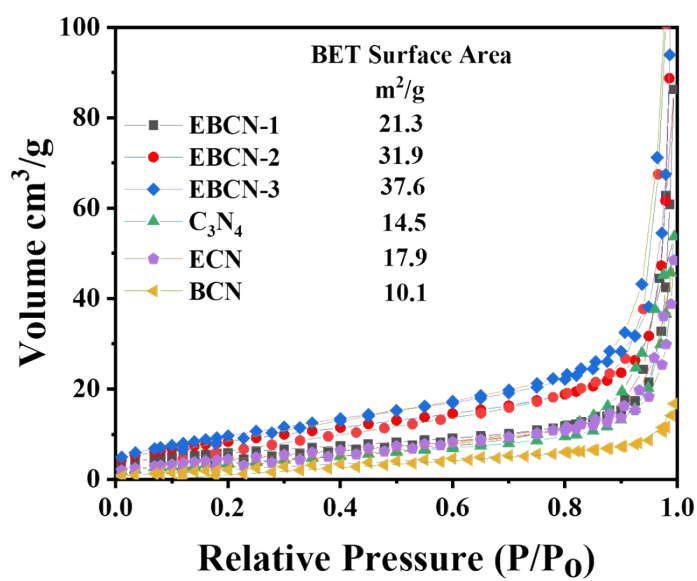
Fig. S6. N_2 sorption isotherms of as-fabricated with the BET surface area data provided

as inset.
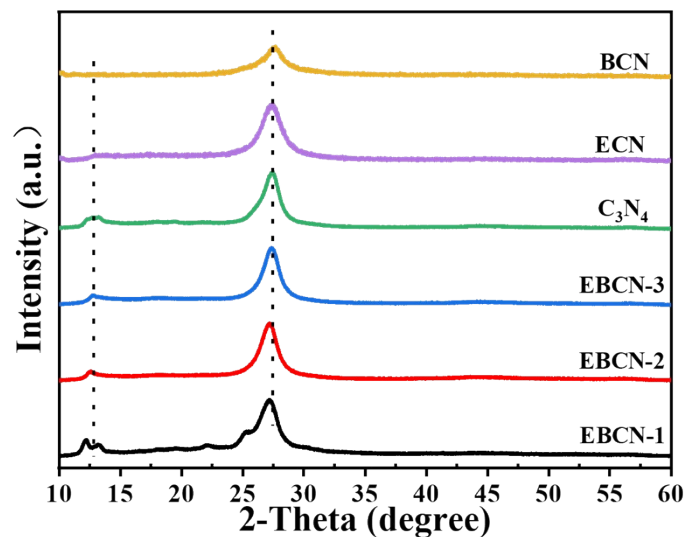
Fig. S7. XRD patterns of as-fabricated samples.
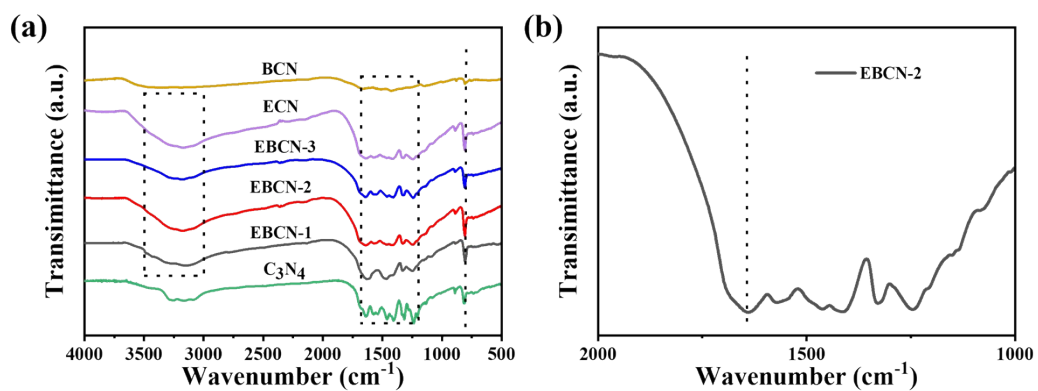
Fig. S8. (a) FTIR patterns of as-fabricated samples, (b) Enlarged FTIR spectrum of EBCN-2.
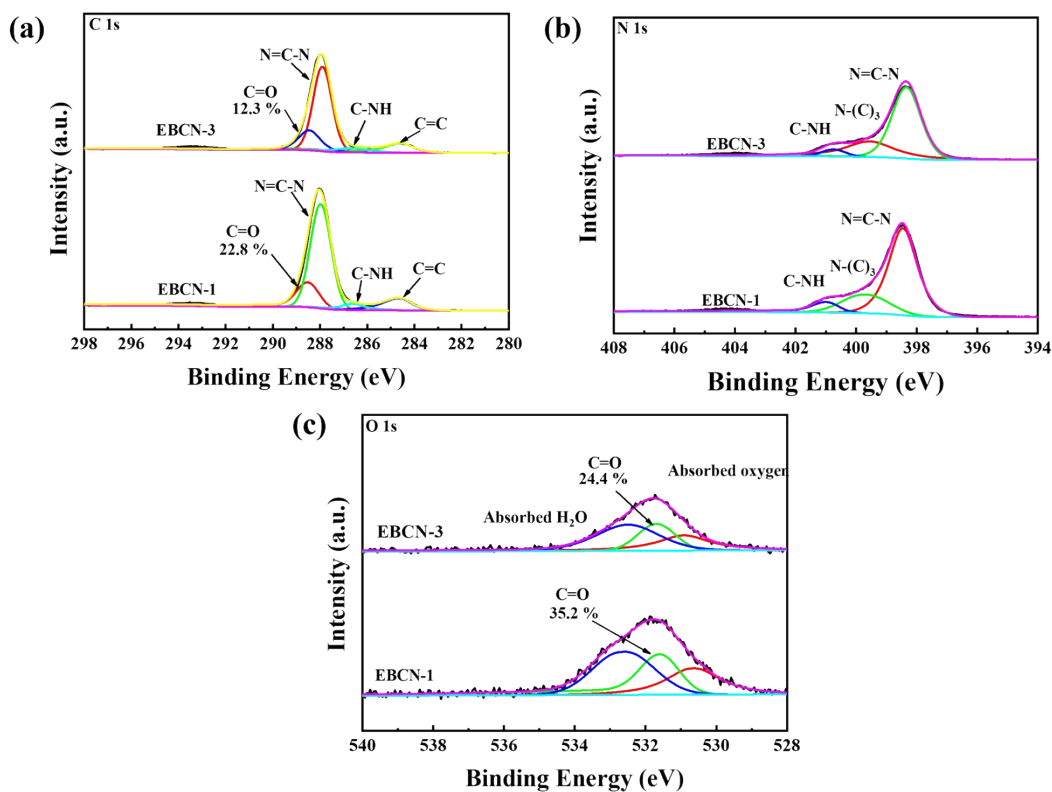
Fig. S9. High-resolution XPS spectra of EBCN-1 and EBCN-3: (a) C 1s, (b) N 1s and (c) O 1s.
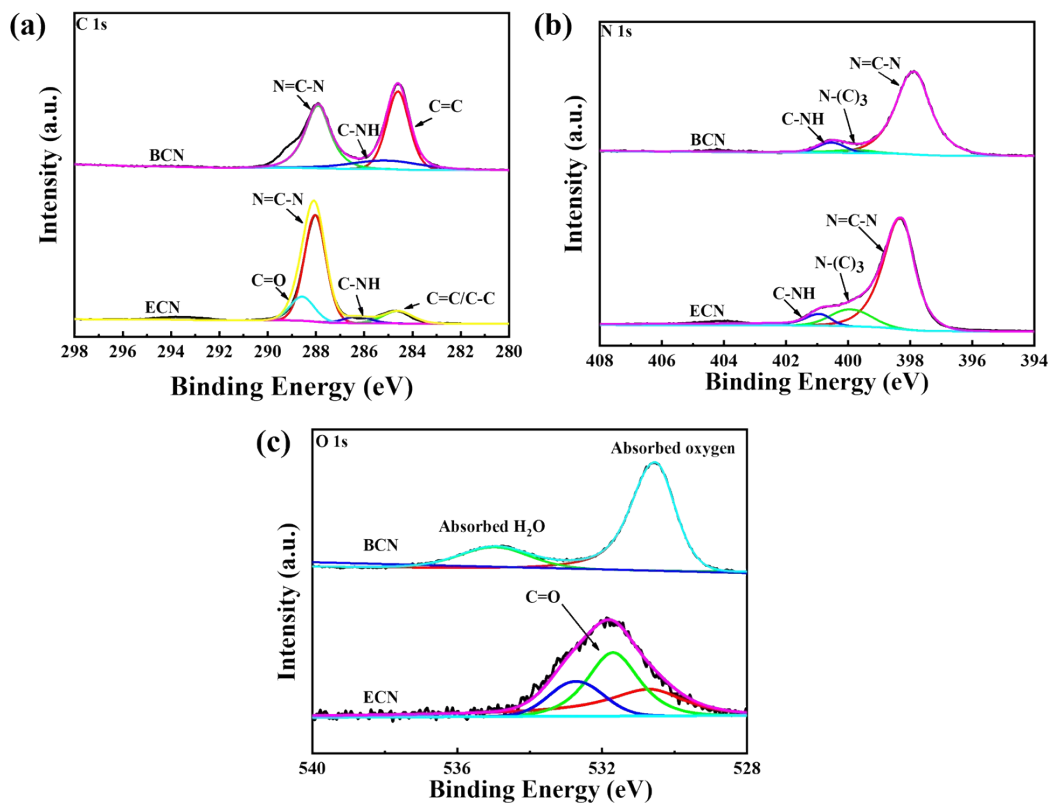
Fig. S10. High-resolution XPS spectra of BCN and ECN catalysts: (c) C 1s, (d) N 1s, (e) O 1s.

As shown in **Fig. S10a**, ECN's C 1s spectra at 288.5, 284.6, 286.2, and 288.0 eV corresponds to O-C=O, C=C, C-NH, and N=C-N bonds,[S9] suggesting that carboxylic groups and C=C linker are effectively grafted on the surface of ECN. The N 1s peaks of ECN at 398.2, 399.9, and 400.9 eV were related to the C-N=C, N-(C)$_3$, and C-NH bonds, respectively (**Fig. S10b**).[S10] The O 1s spectrum also reveals three peaks at 530.7, 531.7 and 532.7 eV, which are attributed to absorbed oxygen, O-C=O and absorbed H$_2$O.[S11] The peaks detected at 284.6, 286.2 and 287.9 eV corresponding to C=C, C-NH, and N=C-N bonds.[S9] The N 1s peaks of BCN at 397.9, 399.7, and 400.5 eV were related to the C-N=C, N-(C)$_3$, and C-NH bonds,[S10] respectively. Above all, the results indicated that the ECN and BCN had been effectively prepared.
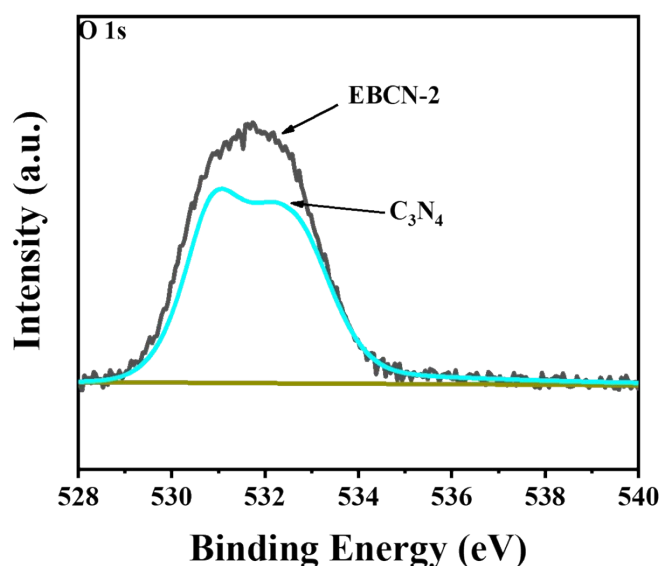
Fig. S11. O 1s high-resolution spectra of EBCN-2 and C$_3$N$_4$.
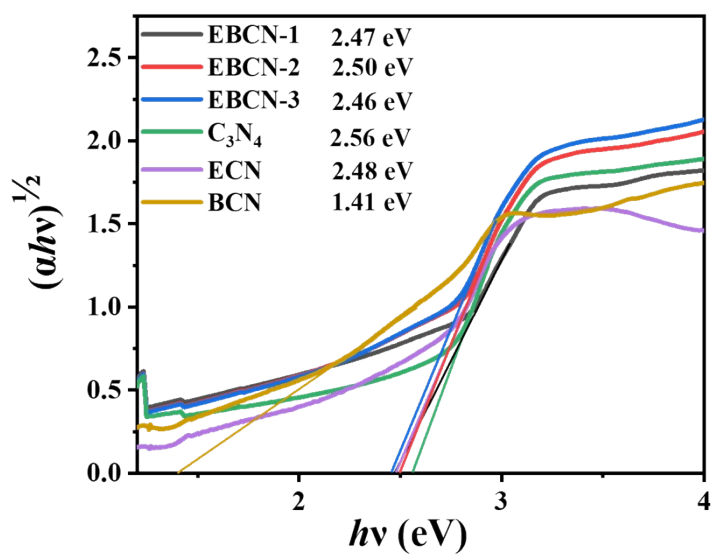
Fig. S12. The corresponding Tauc plots of fabricated samples.
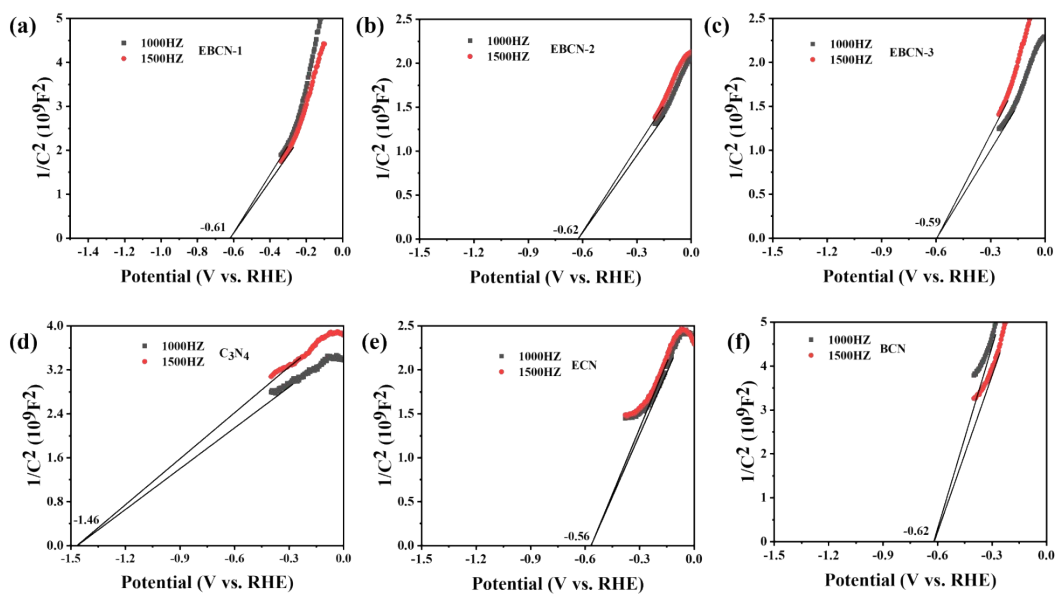
Fig. S13. Mott-Schottky plots of fabricated samples: (a) EBCN-1, (b) EBCN-2, (c) EBCN-3, (d) C_3N_4, (e) ECN and (f) BCN.
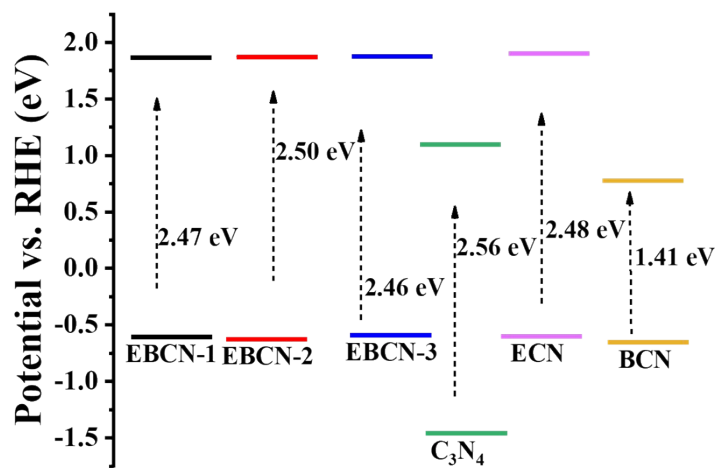
Fig. S14. Schematic diagram of the electronic band structure of fabricated samples.
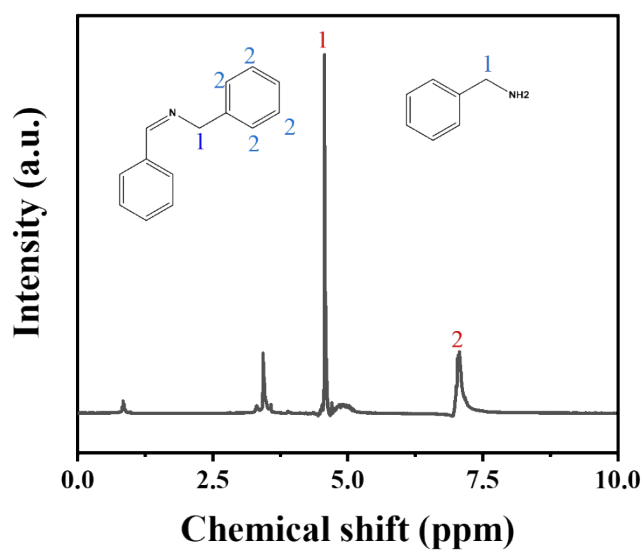
Fig. S15. ^{1}H NMR spectrum of benzylamine oxidation products.
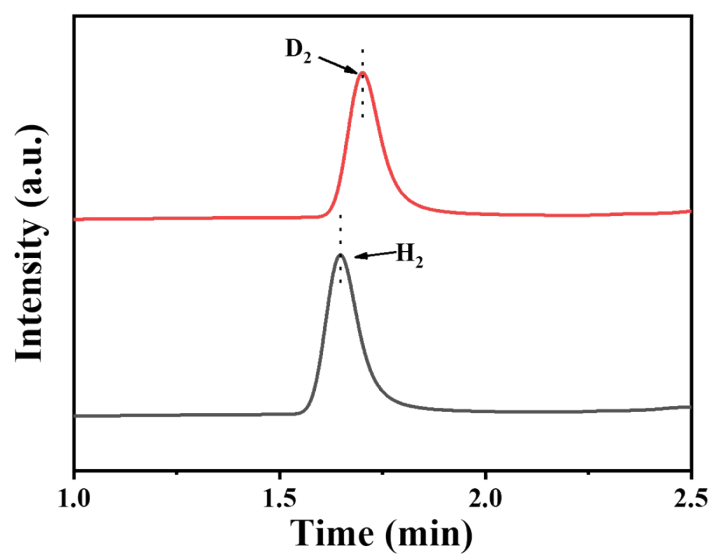
Fig. S16. The D_2O hydrogen production experiment of EBCN-2.
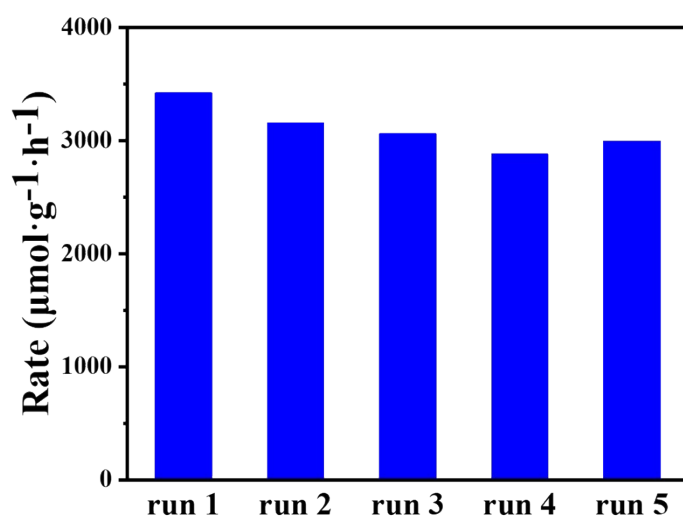
Fig. S17. Cycling performance of EBCN-2 toward selective benzylamine oxidation.
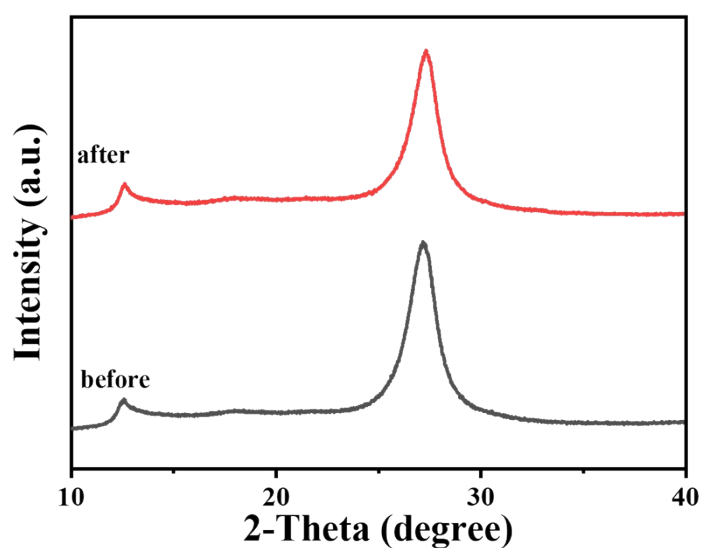
Fig. S18. XRD pattern of EBCN-2 before and after five cycles for photocatalytic H_2 production with selective benzylamine oxidation.
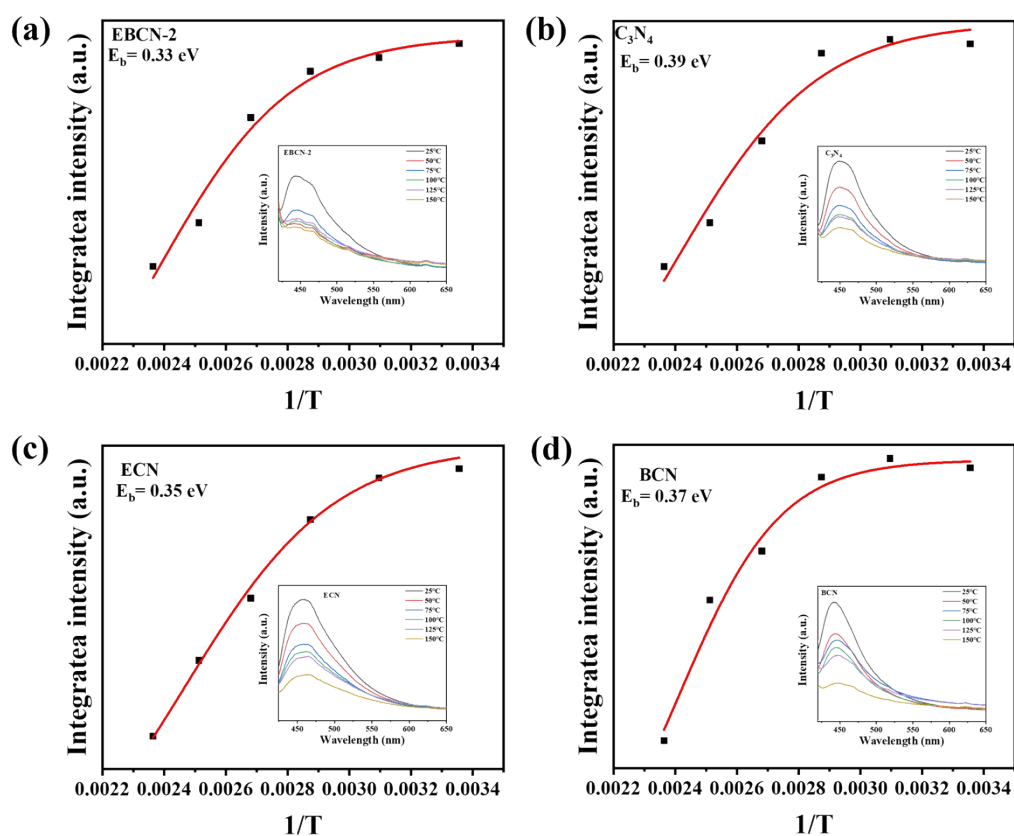
Fig. S19. Integrated PL emission intensity as a function of temperature from 298 to 423 K of (a) EBCN-2, (b) C_3N_4, (c) ECN and (d) BCN
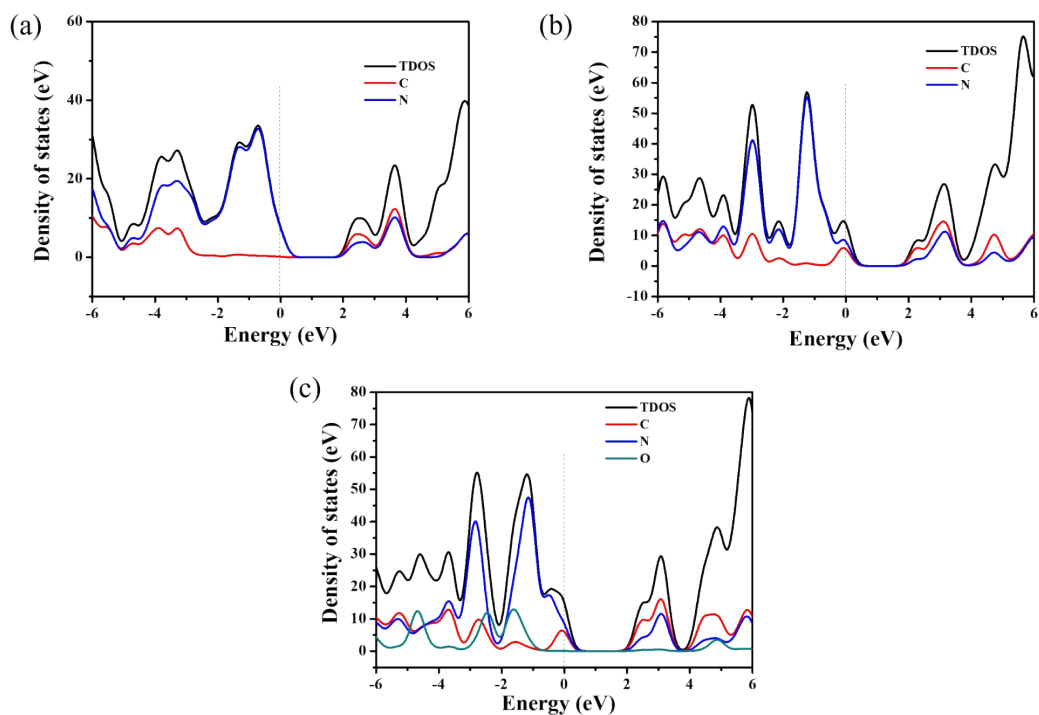
Fig. S20. the DOS of (a) C_3N_4, (b) ECN and (c) BCN.
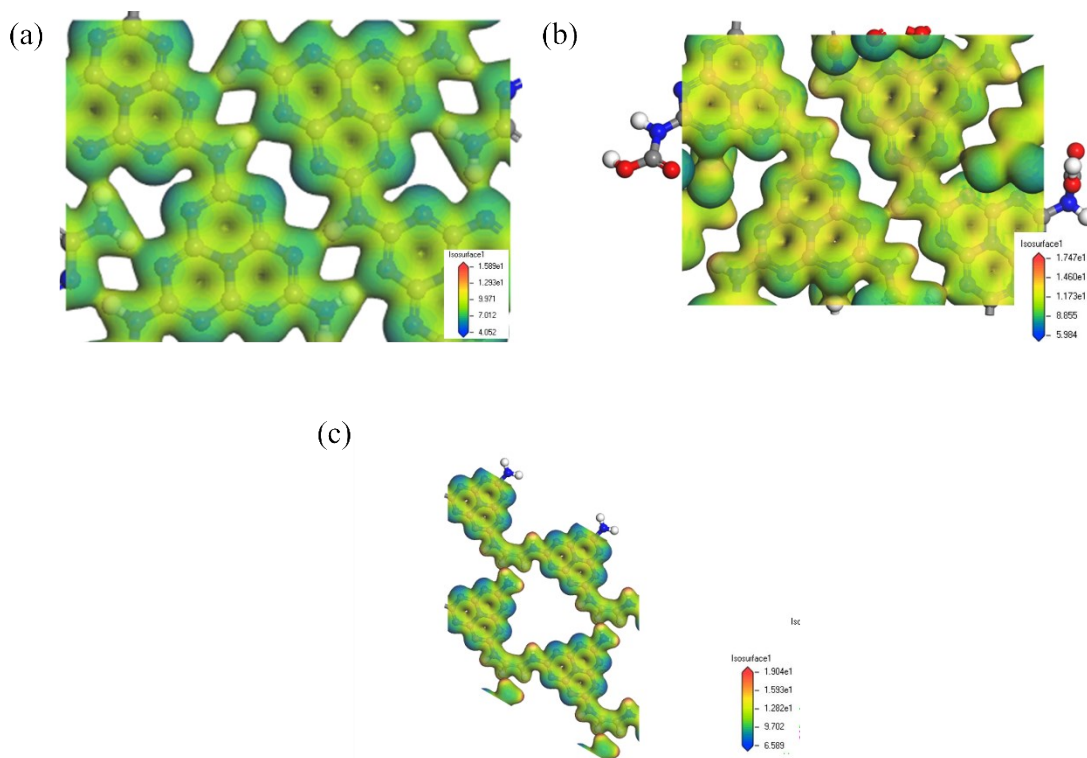
Fig. S21. The charge density of (a) C_3N_4, (b) ECN and (c) BCN.
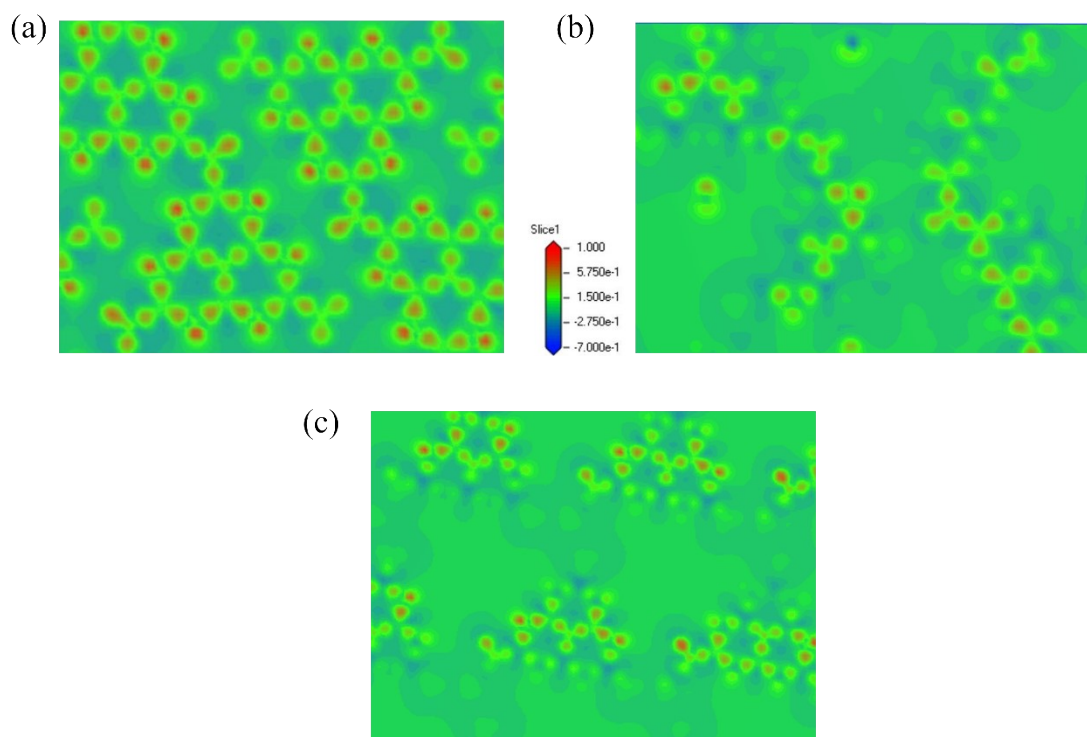
Fig. S22. The differential charge density of (a) C$_3$N$_4$, (b) ECN and (c) BCN.
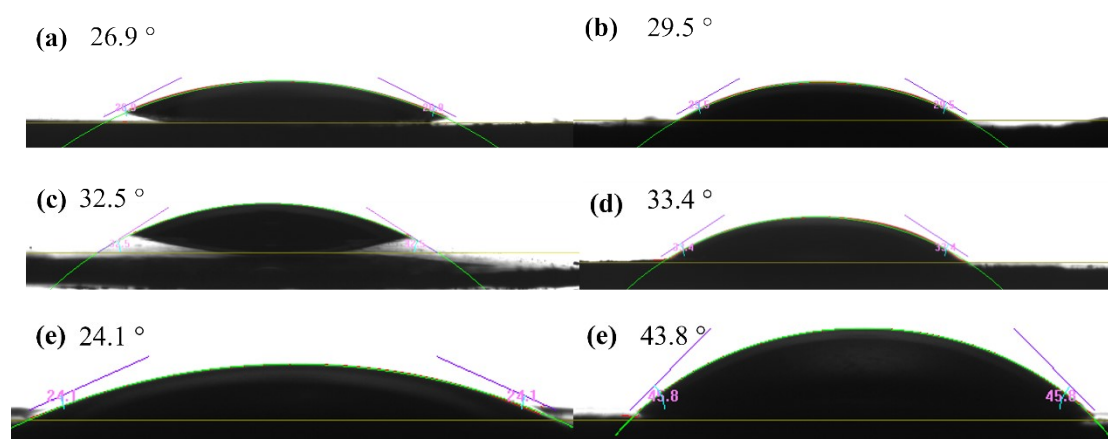
Fig. S23. Contact-angle of water on the surface of (a) EBCN-1, (b) EBCN-2, (c) EBCN-3, (d) C$_3$N$_4$, (e) ECN and (f) BCN.

(a) 14.8 ° **(b)** 17.1 °

(c) 18.4 ° **(d)** 23.4 °

(e) 13.2 ° **(f)** 29.3 °
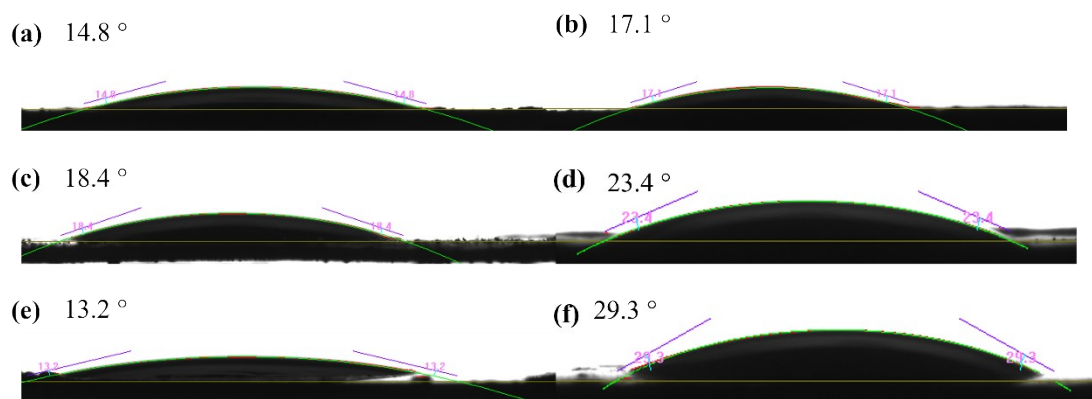
Fig. S24. Contact-angle of benzylamine on the surface of (a) EBCN-1, (b) EBCN-2, (c) EBCN-3, (d) C_3N_4, (e) ECN and (f) BCN.
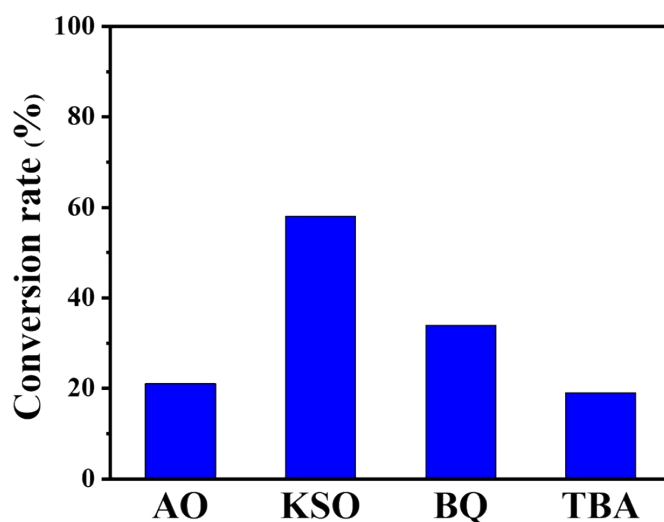
Fig. S25. Photocatalytic selective oxidation of benzylamine over EBCN-2 with or without a scavenger. Ammonium oxalate (AO), Potassium persulfate (KSO), p-benzoquinone (BQ) and tert-butanol (TBA) as scavengers for the hole (h^+), electron (e^-), superoxide radical ($O2^{\bullet-}$) and hydroxyl radical ($\cdot OH$) trapping, respectively.
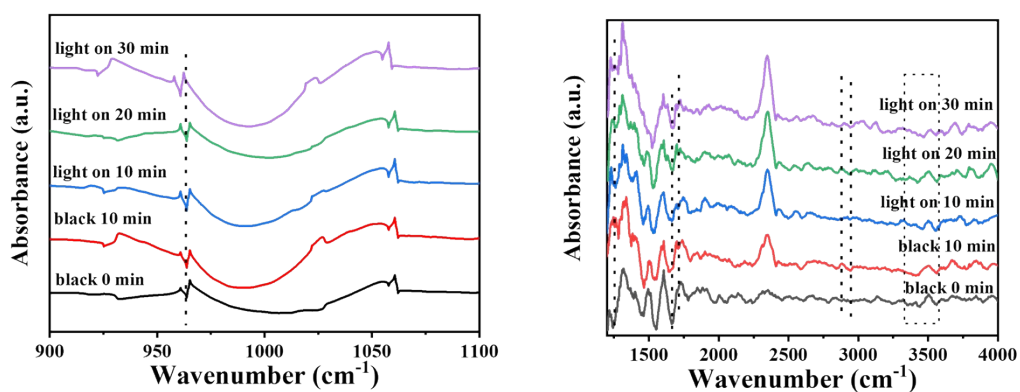
Fig. S26. *in situ* FT-IR of EBCN-2 under water and benzylamine.
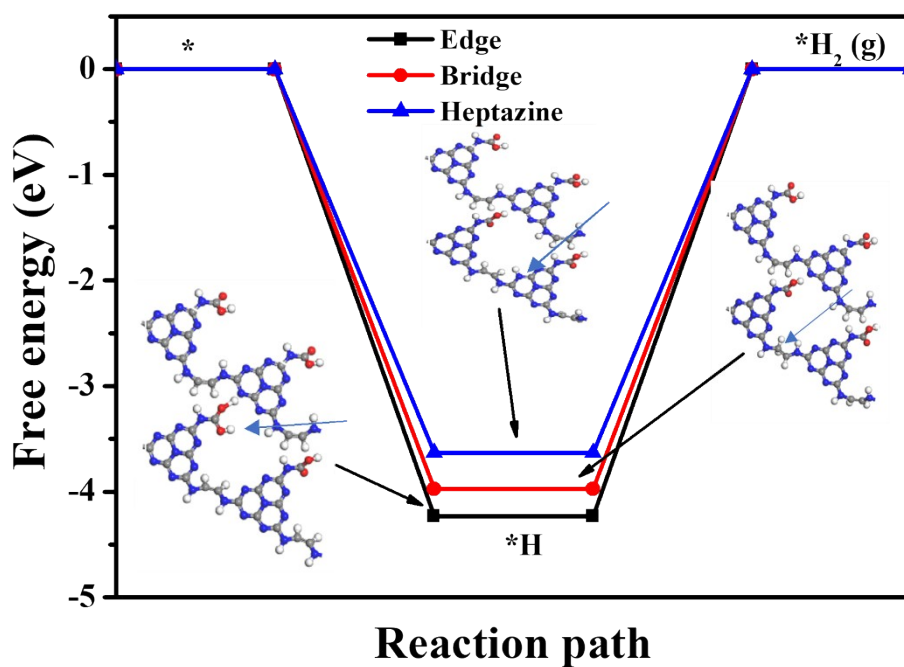
Fig. S27. DFT-calculated Gibbs free energy of hydrogen adsorption.
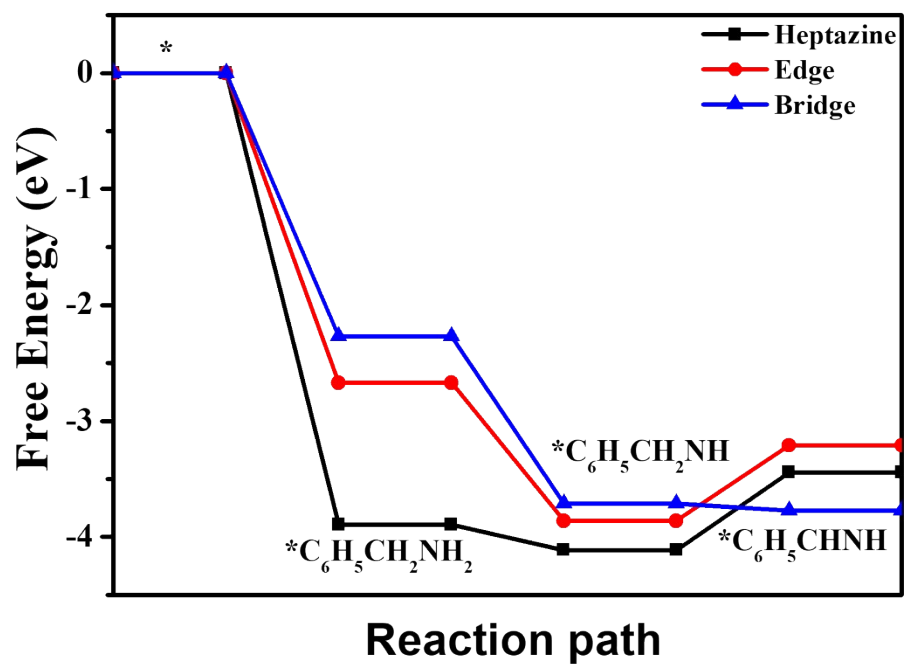
Fig. S28. DFT-calculated Gibbs free energy of selective amines oxidation.
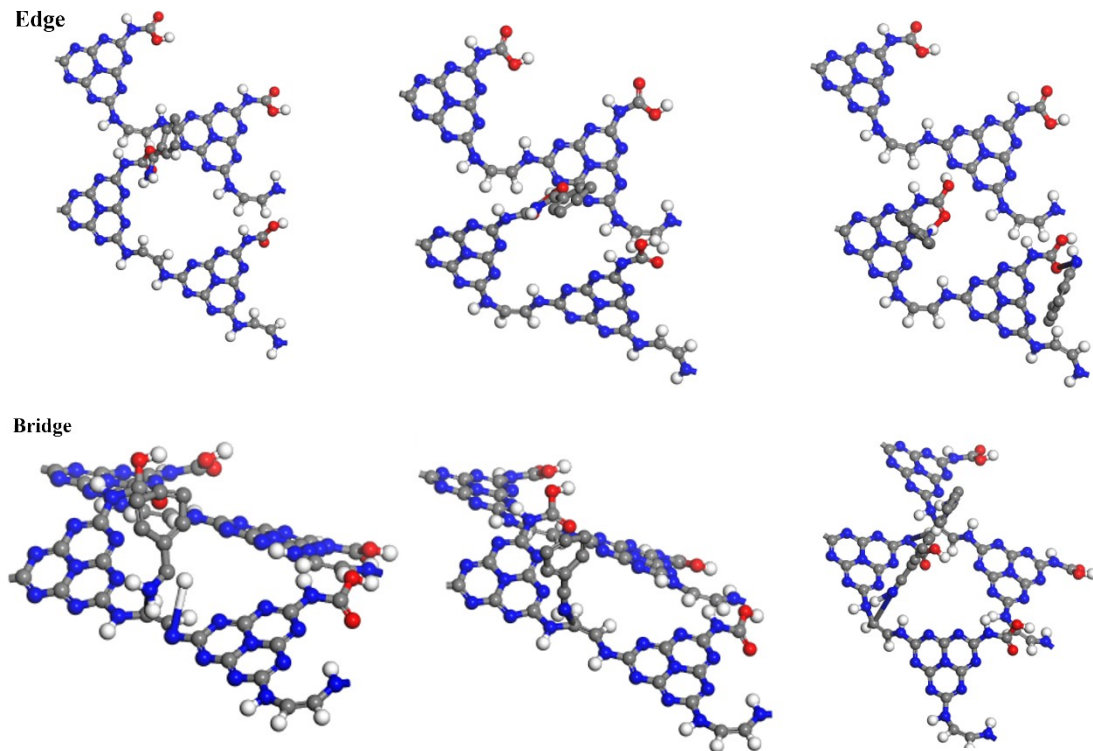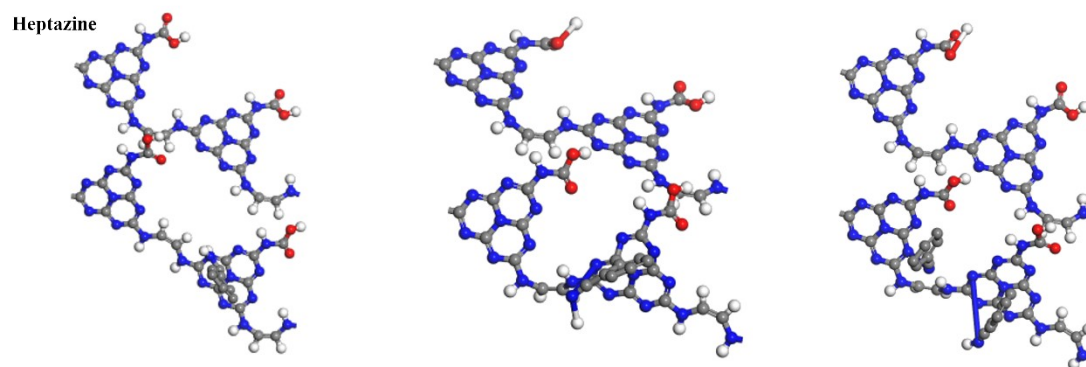
Fig. S29. The geometrical configuration for benzylamine dehydrogenation.

Reference:

S1 H. Liu, C. Xu, D. Li, H.-L. Jiang, *Angew. Chem. Int. Ed*., 2018, **57**, 5379-5383.

S2 T. Wang, X. Tao, X. Li, K. Zhang, S. Liu, B. Li, Small., 2021, **17**, e2006255.

S3 H. Wang, P. Hu, J. Zhou, M.B.J. Roeffaers, B. Weng, Y. Wang, H. Ji, *J. Mater. Chem. A*, 2021, **9**, 19984-19993.

S4 V.W.-h. Lau, M.B. Mesch, V. Duppel, V. Blum, J. Senker, B.V. Lotsch, *J. Am. Chem. Soc*., 2015, **137**, 1064-1072.

S5 Y.A. Workie, Sabrina, T. Imae, M.P. Krafft, *ACS Biomater. Sci. Eng*., 2019, **5**, 2926-2934.

S6 G. Zhang, Y. Xu, C. He, P. Zhang, H. Mi, *Appl. Catal. B Environ.*, 2021, **283**, 119636.

S7 S. Yang, Q. Wang, Q. Wang, G. Li, T. Zhao, P. Chen, F. Liu, S.-F. Yin, *J. Mater. Chem. A*, 2021, **9**, 21732-21740.

S8 P. Kumar, E. Vahidzadeh, U.K. Thakur, P. Kar, K.M. Alam, A. Goswami, N. Mahdi, K. Cui, G.M. Bernard, V.K. Michaelis, K. Shankar, *J. Am. Chem. Soc*., 2019, **141**, 5415-5436.

S9 Z. Gao, K. Chen, L. Wang, B. Bai, H. Liu, Q. Wang, *Appl. Catal. B Environ.*, 2020, **268**, 118462.

S10 W. Zhao, Y. Li, P. Zhao, L. Zhang, B. Dai, J. Xu, H. Huang, Y. He, D.Y.C. Leung, *Chem. Eng. J.*, 2021, **405**, 126555.

S11 J. Meng, X. Wang, Y. Liu, M. Ren, X. Zhang, X. Ding, Y. Guo, Y. Yang, *Chem. Eng. J.*, 2021, **403**, 126354.